IEEE Photonics Journal
An IEEE Photonics Society Publication

In-Situ Measurement of Backscattering in Hollow-Core Fiber Based Resonant Cavities

Volume 9, Number 4, August 2017

Alexia Ravaille
Gilles Feugnet
Ihsan Fsaifes
Assaad Baz
Benoît Debord
Frédéric Gérôme
George Humbert
Fetah Benabid
Fabien Bretenaker, ***Member, IEEE***

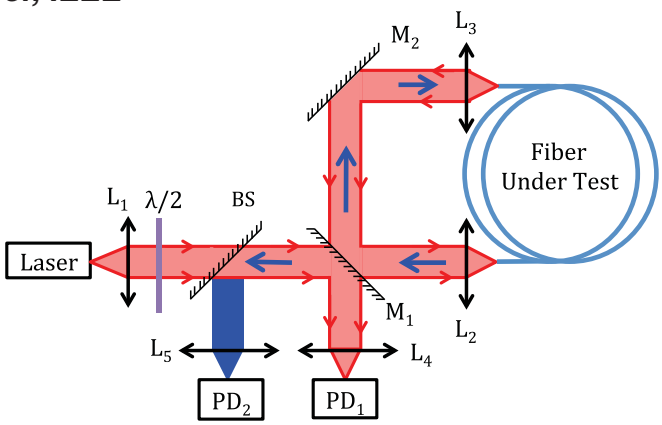

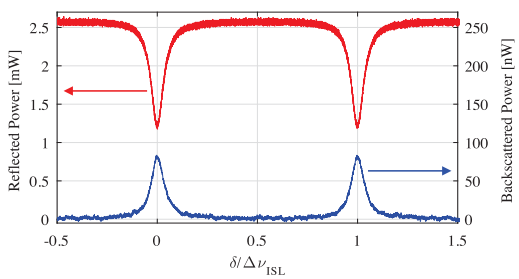

DOI: 10.1109/JPHOT.2017.2713441

In-Situ Measurement of Backscattering in Hollow-Core Fiber Based Resonant Cavities

Alexia Ravaille,[1,2,3] Gilles Feugnet,[1] Ihsan Fsaifes,[2] Assaad Baz,[4] Benoît Debord,[4] Frédéric Gérôme,[4] George Humbert,[4] Fetah Benabid,[4] and Fabien Bretenaker,[2] *Member, IEEE*

[1]Thales Research & Technology, Palaiseau 91120, France
[2]Laboratoire Aimé Cotton, CNRS, Université Paris-Sud, ENS Paris-Saclay, Université Paris-Saclay, Orsay 91400, France
[3]Thales Avionics, Châtellerault 86100, France
[4]GPPMM Group, XLIM Research Institute, CNRS, Université de Limoges, Limoges 87032, France

DOI:10.1109/JPHOT.2017.2713441

Manuscript received March 21, 2017; revised June 1, 2017; accepted June 5, 2017. Date of publication June 8, 2017; date of current version June 23, 2017. This work was supported in part by the Agence Nationale de la Recherche under Awards ANR-13-BS03-0007 and ANR-11-CHEX-0009, and in part by the European Space Agency. Corresponding author: Fabien Bretenaker (e-mail: fabien.bretenaker@lac.u-psud.fr).

Abstract: We measure the light backscattered by resonant optical cavities based on two types of hollow-core photonic bandgap fibers, namely, 7-cell and 19-cell fibers. The measurement of the intensity backscattered by the cavity at resonance permits to deduce the value of the fiber backscattering coefficient. We find backscattering coefficients of the order of 2.0×10^{-6} and 1.0×10^{-6} m^{-1} for the 7-cell and 19-cell fibers, respectively, two orders of magnitude larger than the one for standard solid-core single-mode fiber.

Index Terms: Gyroscopes, resonators, photonic crystal fibers.

1. Introduction

For the last few years, there has been a renewed interest for the resonant fiber optic gyroscope (R-FOG), due in particular to the recent progress of hollow-core photonic crystal fibers (HC-PCF) [1]. Indeed, R-FOGs using conventional silica fibers are limited by several noises, in particular Kerr-effect-induced drift [2] and temperature-driven polarization instability [3], which prevent them from becoming a commercial competitor of the interferometric fiber optic gyroscope (I-FOG). More precisely, the main source of bias in a conventional R-FOG arises from the propagation of monochromatic light in a glass medium, leading to an intensity dependent refractive index [1]. It has been shown that using HC-PCF as the sensing coil permits light to propagate mainly in air, thus making the R-FOG less sensitive to such Kerr non-linearities [4]. Besides, it has been known since [5] that backscattering limits the accuracy of R-FOGs. Indeed, it is responsible for the lock-in phenomenon that prevents the R-FOG from measuring slow angular velocities. While the backscattering in standard silica fiber is well known, there is no specific instrument developed to measure such a parameter in HC-PCF. To date, to the best of our knowledge, there are only two direct measurements of backscattering in HC-PCF: one performed using a commercial reflectometer (Luna Technology)

[6] and one extracted from Optical Frequency Domain Reflectometer (OFDR) measurements [7]. These two measurements were performed with the same commercial 7-cell HC-PCF from NKT. However, different types of HC-PCFs can be considered for application to R-FOG. For example, recently, 19-cell photonic bandgap HC-PCF was found to be a good candidate [8]. The aim of the present paper is thus to compensate the lack of information concerning backscattering in HC-PCFs by proposing a simple in-situ measurement method based on measuring the backscattered power directly in a R-FOG configuration. The system developed here allows us to compare different types of HC-PCF and to measure backscattering over different lengths. The proposed method also offers the benefit of requiring only a few meters of fiber. This is important in terms of cost and also when such fibers are difficult to manufacture or exhibit variations of their parameters along propagation.

The paper is organized as follows. In Section 2, we derive the theoretical expressions that relate the intensity reflected by the cavity to the fiber backscattering coefficient. Section 3 describes the experimental setup. Finally, Section 4 presents the experimental results for different types of fibers and discusses the accuracy of these measurements.

2. Theory

When coherent light is launched into an optical fiber, a fraction of its intensity is scattered in all directions due to Rayleigh scattering. The backscattered fraction of the intensity launched into the fiber of length L is given by [9]

$$\alpha_{\mathrm{BS}} = \alpha_{\mathrm{S}} S \frac{1 - \mathrm{e}^{-2\alpha L}}{2\alpha} , \tag{1}$$

where α_{S} is the Rayleigh scattering coefficient of the fiber, S the recapture factor [9], and α the total attenuation coefficient of the fiber. If L is small enough for the total attenuation to be small, i.e. $\alpha L \ll 1$, then (1) reduces to:

$$\alpha_{\mathrm{BS}} \simeq \alpha_{\mathrm{S}} S L . \tag{2}$$

If such a fiber of length L is used to build a ring resonator of area A, the lock-in threshold for the rotation rate that can be observed with this cavity in a passive resonant gyro architecture is given by [5], [10]:

$$\Omega_{\mathrm{LI}} = \frac{c\lambda\sqrt{\alpha_{\mathrm{BS}}}}{4\pi A} , \tag{3}$$

where c is the velocity and λ the wavelength of light. Since in the following we consider only hollow-core fibers, those quantities are taken in vacuum. From (3) we can thus see that fiber backscattering has a direct impact on the performance of the gyro.

Rather than measuring the fiber backscattering coefficient using reflectometers [6], [7], we decide here to perform a measurement in a gyrometer resonant cavity. Since we want to compare different fibers, we choose a semi-bulk cavity architecture, as shown in Fig. 1.

This cavity is closed with mirrors M_1 (cavity output coupler) and M_2 (a highly reflecting mirror) and contains the fiber under test, together with its coupling optics. We call r_1 (resp. r_2) and t_1 (resp. t_2) the amplitude reflection and transmission coefficients of mirror M_1 (resp. M_2) and t the amplitude transmission coefficient for the intracavity fiber including both injection losses and fiber attenuation. If one excites the cavity with a field with complex amplitude E_0 (intensity I_0) incident on mirror M_1, the field amplitude inside the cavity, just after mirror M_1, is

$$E_{\mathrm{cav}} = \frac{t_1}{1 - r_1 r_2 t \exp\left(\frac{\mathrm{i}2\pi\delta}{\Delta\nu_{\mathrm{ISL}}}\right)} E_0 , \tag{4}$$

where δ is the frequency detuning with respect to resonance and $\Delta\nu_{\mathrm{ISL}}$ the cavity free spectral range. The field reflected by the cavity is the sum of the incident field directly reflected from mirror

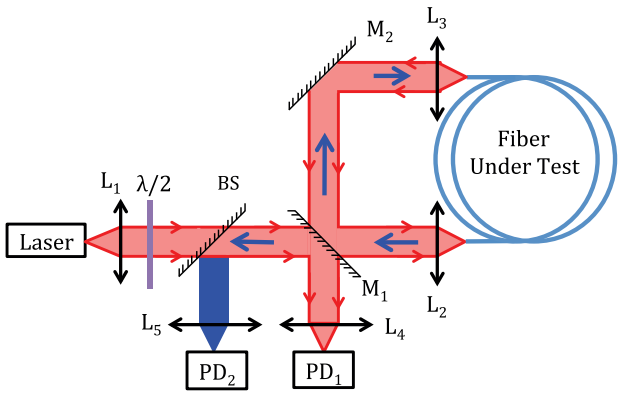

Fig. 1. Experimental setup aimed at measuring light backscattered from the fiber resonator. The laser frequency can be linearly swept to probe the resonator resonances. M_1, M_2: mirrors. PD_1, PD_2: photodetectors. BS: beamsplitter.

M_1 and the fraction of the intracavity field of (4) that is transmitted by mirror M_1:

$$E_R = -r_1 E_0 + t_1 t r_2 \exp\left(\frac{i2\pi\delta}{\Delta\nu_{ISL}}\right) E_{cav}. \tag{5}$$

The reflected intensity is obtained by taking the square modulus of (5), which can be written in the following form:

$$I_R = I_0(r_1^2 + t_1^2)\left\{1 - \frac{1 - \frac{\left[r_1 - (r_1^2+t_1^2)tr_2\right]^2}{(1-r_1r_2t)^2(r_1^2+t_1^2)}}{1 + \frac{4r_1r_2t}{(1-r_1r_2t)^2}\sin^2\left(\frac{\pi\delta}{\Delta\nu_{ISL}}\right)}\right\}, \tag{6}$$

where $(r_1^2 + t_1^2)$ might be different from 1 because of the losses of the mirror. The existence of backscattering given by (2) inside the cavity will convert a fraction of the intracavity field of (4) into a counterpropagating intracavity field. This field (namely $\sqrt{\alpha_{BS}}E_{cav}$) is then injected inside the counterpropagating mode as if it were coming from an external source, and the intracavity backscattered field results from the resonance of this injected field [11], [12]. Taking multiple round-trips into account, the intracavity counterpropagating field is thus given by:

$$E_{cav,back} = \frac{\sqrt{\alpha_{BS}}}{1 - r_1r_2t\exp\left(\frac{i2\pi\delta}{\Delta\nu_{ISL}}\right)}E_{cav} = \frac{\sqrt{\alpha_{BS}}\,t_1}{\left[1 - r_1r_2t\exp\left(\frac{i2\pi\delta}{\Delta\nu_{ISL}}\right)\right]^2}E_0\,. \tag{7}$$

At resonance ($\delta = 0$), (7) simplifies, leading to the following expression for the intensity backscattered by the cavity, i.e. at the output of the cavity:

$$\frac{I_{back}(\delta = 0)}{I_0} = \frac{\alpha_{BS}t_1^4}{(1 - r_1r_2t)^4}. \tag{8}$$

Equation (8) shows that the measurement of the intensity backscattered by the cavity at resonance permits to determine the fiber backscattering coefficient α_{BS}, provided we know the values of the cavity parameters r_1, r_2, t_1, and t. However, (5) shows that these parameters can be experimentally determined by measuring the reflection spectrum of the cavity, as explained in the following section.

3. Experimental Setup

The measurement of the intensities backscattered and reflected by the resonant cavity is performed as shown in Fig. 1. The laser is a commercial 1.55 μm laser (Koheras Adjustik E15 laser from NKT Photonics) with a 100-Hz linewidth and an extremely good frequency stability (frequency noise equal to 65 Hz/$\sqrt{\text{Hz}}$ at 100 Hz and 26 Hz/$\sqrt{\text{Hz}}$ at 1 kHz). The light emitted from this fibered laser (output

TABLE 1
Characteristics of the Investigated Fibers

Fiber type	Length (m)	MFD (μm)	f_1 (mm)
19-cell PBG	25	12	6.24
19-cell PBG	3	12	6.24
7-cell PBG	3	6.3	11

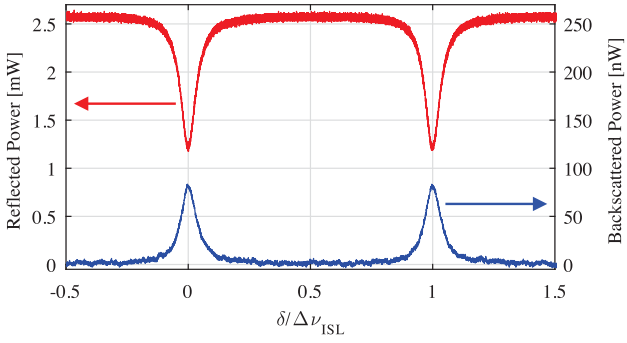

Fig. 2. Experimental evolutions of reflected and backscattered powers when the incident light frequency is scanned. These results were obtained with 25 m of 19-cell PBG fiber provided by GPPMM and an incident power of 2.7 mW.

mode diameter equal to 9.9 μm) is first collimated by lens L_1 (focal length f_1). The resonator consists of the fiber under test, the two lenses L_2 and L_3 of identical focal lengths ($f_2 = f_3 = 6.24$ mm) and the two mirrors M_1 and M_2. To be able to compare the backscattering coefficients of different fibers, those intracavity components (lenses and mirrors) remain the same for all tested fibers. In order to match the external probe laser to the fundamental mode of the cavity, only f_1 is changed. The choice of f_1 is optimized to get the best coupling efficiency for each fiber (see the last column in Table 1).

In all our measurements, we make sure that the cavity transmission spectra and polarization remain unaffected by small environmental changes (fiber curvature, fiber displacement, local strain, . . .). We also check that our cavity alignment procedure leads to reproducible results.

The intensity reflected by the cavity is monitored by PD_1, and one half of the backscattered light intensity is reflected by the beamsplitter BS and monitored by photodiode PD_2. A typical measurement result, while the laser frequency is scanned, is reproduced in Fig. 2.

One can clearly see on this figure that each time the cavity is at resonance, the intracavity backscattering excites a resonant wave propagating in the opposite direction inside the cavity. Such backscattering peaks were also observed in the case of solid core fiber resonators [13]. Here, as explained in Section 2, we use the reflectivity dips to determine the cavity parameters. The result of a fit of one dip of Fig. 2 using (6) is shown in Fig. 3. The quantities which are adjusted during the fit to (6) are actually r_1^2, $r_1^2 + t_1^2$, and $t^2 r_2^2$. For example, the data of Fig. 3 lead to $r_1^2 = 0.895$, $r_1^2 + t_1^2 = 0.966$, and $t^2 r_2^2 = 0.718$. It is worth noticing that, in general, a simple fit of the reflection resonance peak of a cavity has two solutions, corresponding to undercoupling and overcoupling situations [14]. However, here, we know a priori quite well the value of r_1^2, that shows that our cavity is in under coupling regime. This allows us to launch the fitting procedure with initial values close to the actual values of the cavity parameters, ensuring convergence to the correct set of parameters

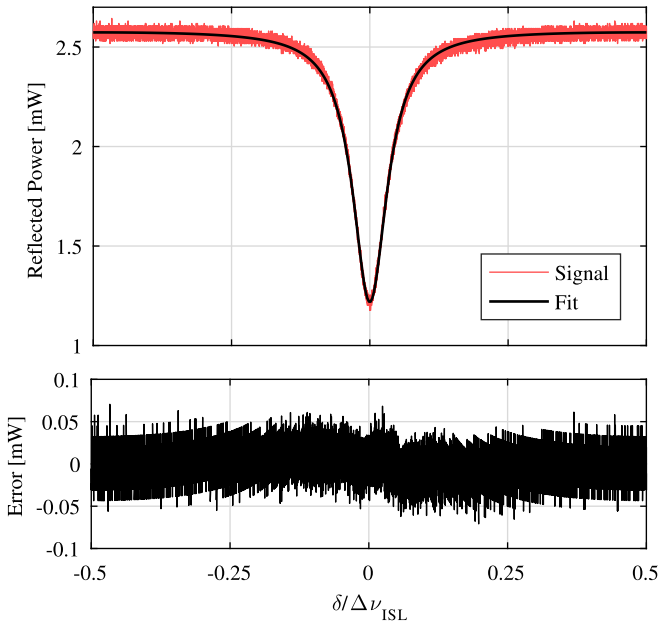

Fig. 3. Fit (black line) of the experimental evolution of the reflected power (red line) of Fig. 2. The lower curve is the residual difference between the signal and the fit.

only. The validity of the fits is thus confirmed by comparing the fitted values of r_1^2 and $r_1^2 + t_1^2$ to their directly measured values, namely $r_1^2 = 0.9$, $r_1^2 + t_1^2 = 0.97$. Once these quantities are known, one can use them in (8) to deduce α_{BS} from the peak of the backscattered spectrum like the one shown in Fig. 2.

Three difficulties make these measurements tricky. The first one is that the backscattered intensity is rather weak, as can be seen by comparing the vertical scales of the two signals of Fig. 2. This means that any spurious reflection from any component that may end up on detector PD_2 will spoil the measurement. We thus made a lot of efforts to mask all spurious reflections coming from all interfaces (for instance by tilting all optical components, in particular the intracavity ones). The second difficulty lies in the polarization alignment of the cavity. Indeed, the light incident on mirror M_1 is vertically polarized. The cavity eigenmodes must hence have the same polarization. In spite of the fact that hollow core fibers are not polarization maintaining, we managed to obtain a stable single polarization inside the cavity by twisting them as demonstrated in [15]. This method allowed us to avoid inserting any intracavity polarizer or waveplates that could have added backscattering. The third difficulty comes from the fact that our measurement procedure is based on the comparison of two strongly different light powers detected with two different detectors. This led us to perform a precise cross calibration. Besides, such detectors can exhibit offsets. In order to cancel the errors arising from these offsets, we made several measurements by varying the power incident on the cavity. We checked that the evolution was linear in the relevant range (see Fig. 4) and we used the slopes of such measurements to extract $I_{\mathrm{back}}(\delta = 0)/I_0$ and thus α_{BS}.

4. Experimental Results

We have explored three different samples of hollow core photonic bandgap fibers, whose characteristics are summarized in Table 1. Two different lengths of 19-cell PBG fiber made at GPPMM were considered: 25 m and 3 m. A 3-m long sample of commercially available 7-cell PBG fiber from NKT was also tested. The measurement results are summarized in Table 2.

We can see that our experimental protocol seems sound because the values of the measured mirror parameters, namely r_1^2 and $r_1^2 + t_1^2$ are reproducible within ± 0.003, and are confirmed by

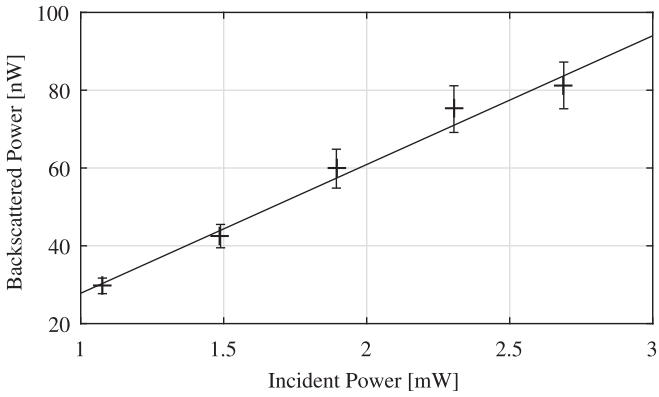

Fig. 4. Example of evolution of the power backscattered by the cavity at resonance as a function of the incident power. The black full line is a linear fit. The slope of the fit is of 33 nW/mW. These results were obtained with the same fiber as in Fig. 3.

TABLE 2
Measurement Results

Fiber Type	Length (m)	r_1^2	$r_1^2 + t_1^2$	$t^2 r_2^2$	Finesse	α_{BS} (measured)	$\alpha_S S$ (measured)	$\alpha_S S$ (literature)
19-cell PBG	25	0.895	0.966	0.718	14.1	2.5×10^{-5}	1.0×10^{-6}	– – –
19-cell PBG	3	0.898	0.960	0.802	19.1	3.9×10^{-6}	1.3×10^{-6}	– – –
7-cell PBG	3	0.899	0.963	0.732	15.0	7.6×10^{-6}	2.5×10^{-6}	1.6×10^{-6} [6]

direct measurements. We can also see that the result we obtain for the 7-cell PBG fiber ($\alpha_S S = 2.5 \times 10^{-6}$ m^{-1}) is of the same order of magnitude as the one mentioned in [6] and extrapolated from the measurements performed in [7], and also in agreement with simulations [16]. Concerning the 19-cell PBG fiber, we find a backscattering coefficient, which is of the same order of magnitude but twice smaller than for the 7-cell fiber. The fact that we obtain similar results for two very different values of the fiber length ($L = 25$ m and $L = 3$ m) shows that the backscattering from intracavity elements (mirrors and lenses) is indeed negligible compared to the one from the fiber. Although the backscattering coefficient is found to be smaller for 19-cell PBG than for 7-cell PBG, we are still far from the ultimate limits mentioned in [4] (7×10^{-10} m^{-1} and 7×10^{-11} m^{-1}, respectively), and two orders of magnitude above the typical backscattering coefficients observed for standard SMF 28 fibers ($\simeq 10^{-8}$ m^{-1}).

Other backscattering measurements were performed on our setup with Kagome HC lattice design fiber from GLOphotonics but were inconclusive due to their unstable multimodal character. As the mode at the output of the fiber was strongly modified by any local pressure on the fiber or slight displacement of it, it was not possible to obtain reproducible measurements. Indeed, different mode profiles must lead to different overlap with the surrounding glass and then to different backscattering coefficients.

5. Conclusion

In conclusion, we have performed backscattering measurements on a cavity based on two types of HC-PCF, namely 19-cell and 7-cell PBG fibers, that are aimed at being used to build R-FOG

cavities. These measurements confirm the order of magnitude of the backscattering coefficient for 7-cell fiber [6], [7], [15] and show that the backscattering coefficient is slightly smaller, but of the same order of magnitude, for 19-cell PBG fiber. These backscattering coefficients are two orders of magnitude larger than the one usually observed for standard single-mode fiber, showing that lock-in threshold should be a difficult issue with such fibers. Finally, these results confirm that a new types of servo control architectures [17] aiming at measuring the cavity rotation may prove instrumental to cancel the effect of backscattering on the lock-in zone.

Acknowledgement

The work of AR, GF, IF, and FB has been realized in the framework of the joint research laboratory between Laboratoire Aimé Cotton and Thales Research & Technology.

References

[1] G. A. Sanders, L. K. Strandjord, and T. Qiu, "Hollow core fiber optic ring resonator for rotation sensing," in *Proc. OSA Opt. Fiber Sensors*, Cancun, Mexico, Oct. 2006, Paper ME6.
[2] K. Iwatsuki, K. Hotate, and M. Higashiguchi, "Kerr effect in an optical passive ring-resonator gyro," *J. Lightw. Technol.*, vol. LT-4, no. 6, pp. 645–651, Jun. 1986.
[3] H. Ma, Z. Chen, Z. Yang, X. Yu, and Z. Jin, "Polarization-induced noise in resonator fiber optic gyro," *Appl. Opt.*, vol. 51, no. 28, pp. 6708–6717, 2012.
[4] M. A. Terrel, M. J. F. Digonnet, and S. Fan, "Resonant fiber optic gyroscope using an air-core fiber," *J. Lightw. Technol.*, vol. 30, no. 7, pp. 931–937, Apr. 2012.
[5] F. Zarinetchi and S. Ezekiel, "Observation of lock-in behavior in a passive resonator gyroscope," *Opt. Lett.*, vol. 11, no. 6, pp. 401–403, 1986.
[6] S. Lloyd, V. Dangui, M. Digonnet, S. Fan, and G. S. Kino, "Measurement of reduced backscattering noise in laser-driven fiber optic gyroscopes," *Opt. Lett.*, vol. 25, no. 2, pp. 121–123, 2010.
[7] M. Wegmuller, M. Legré, N. Gisin, T. Hansen, C. Jakobsen, and J. Broeng, "Experimental investigation of the polarization properties of a hollow core photonic bandgap fiber for 1550 nm," *Opt. Exp.*, vol. 13, no. 5, pp. 1457–1467, 2005.
[8] I. Fsaifes *et al.*, "Hollow-core photonic-bandgap fiber resonator for rotation sensing," in *Proc. OSA Conf. Lasers Electro-Opt.*, San José, CA, USA, Jun. 2016, Paper SM2P.4.
[9] P. Gysel and R. K. Staubli, "Statistical properties of Rayleigh backscattering in single-mode fibers," *J. Lightw. Technol.*, vol. 8, no. 4, pp. 561–567, Apr. 1990.
[10] R. J. C. Spreeuw, J. P. Woerdman, and D. Lenstra, "Photon band structure in a Sagnac fiber-optic ring resonator," *Phys. Rev. Lett.*, vol. 61, no. 3, pp. 318–321, 1988.
[11] T. J. Kippenberg, S. M. Spillane, and K. J. Vahala, "Modal coupling in traveling-wave resonators," *Opt. Lett.*, vol. 27, no. 19, pp. 1669–1671, 2002.
[12] S. Trebaol, Y. Dumeige, and P. Féron, "Ringing phenomenon in coupled cavities: Application to modal coupling in whispering-gallery-mode resonators," *Phys. Rev.*, vol. 81, 2010, Art. no. 043828.
[13] H. Ma, X. Chang, Z. Yang, and Z. Jin, "Full investigation of the backscattering in resonator fiber optic gyro," *Opt. Commun.*, vol. 284, no. 19, pp. 4480–4484, 2011.
[14] Y. Dumeige, S. Trebaol, L. Ghişa, T. K. N. Nguyên, H. Tavernier, and P. Féron, "Determination of coupling regime of high-Q resonators and optical gain of highly selective amplifiers," *J. Opt. Soc. Amer. B*, vol. 25, no. 12, pp. 2073–2080, 2008.
[15] M. Terrel, M. J. F. Digonnet, and S. Fan, "Polarization controller for hollow-core fiber," *Opt. Lett.*, vol. 32, no. 11, pp. 1524–1526, 2007.
[16] V. Dangui, M. J. F. Digonnet, and G. S. Kino, "Modeling of the propagation loss and backscattering in air-core photonic-bandgap fibers," *J. Lightw. Technol.*, vol. 27, no. 17, pp. 3783–3789, Sep. 2009.
[17] S. Schwartz, G. Feugnet, and F. Bretenaker, "Gyromètre optique passif à trois faisceaux," Patent EP2857797 A1, 2013.